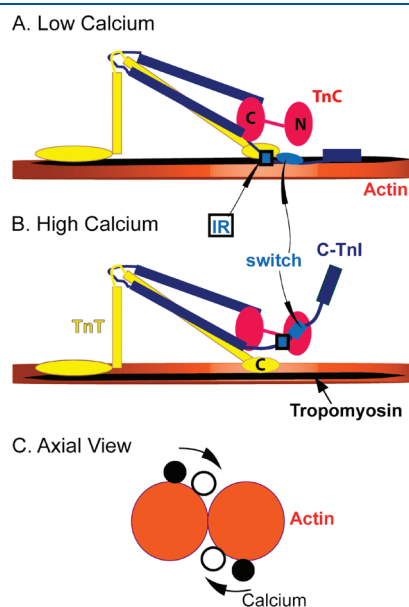




Thus, the effects of bepridil on calcium sensitivity may depend on other members of the regulatory complex.

In this work, to understand how bepridil affects troponin at an atomic level, four systems of troponin were investigated



**Figure 1.** Schematic view of the troponin–tropomyosin–actin complex. Actin is in orange, tropomyosin in black, TnI in blue, TnT in yellow, and TnC in red. The switch segment of TnI is shown either as a light blue ellipse or as a rectangle. The inhibitory region of TnI (IR) is shown as a blue and black rectangle. (A) Calcium-free state.<sup>13</sup> (B) Calcium-bound state.<sup>13</sup> (C) Tropomyosin position change with calcium.<sup>2</sup>

using MD simulations based on available structures. The four systems, as shown in Figure 2, contain different parts of troponin. Each system was simulated with and without bepridil. Since the hydrophobic pocket which is exposed on TnC by calcium binding is the binding site for bepridil, all structures used in the simulation have calcium. The theoretical aspects of this work were complemented by experimental measurements of effects of bepridil on ATPase activities and the rates of  $\text{Ca}^{2+}$  detachment.

## II. METHODS AND MATERIALS

**Simulation Systems.** The details of the four systems are listed in Table 1. System 1 was based on the NMR complex structure that contains the N-domain of TnC<sub>1–89</sub>, the switch segment of TnI<sub>147–163</sub>, and bepridil (PDB ID: 1LXF).<sup>12</sup> Bepridil was removed for the simulation in system 1A. The initial structure for system 2 was based on the X-ray structure (PDB ID: 1J1D)<sup>13</sup> by removing the TnI and TnT segments from the structure. In order to place the bepridil in the binding pocket of TnC in system 2B, the bepridil complex structure of 1LXF was first aligned to the N-domain of this system and these coordinates were used to dock the ligand in the pocket. System 3 was modeled by using the N and C domains from the system 2 model and aligning to the 1LXF model. The TnI segment (147–163, 1LXF) coordinates were used after the alignment for system 3 and the bepridil coordinates were used for placing the ligand in the pocket for system 3B. The initial structure for system 4 was the complete model of 1J1D with the TnI linker connecting the switch segment with the two large helices built using homology module in Insight II.<sup>14,15</sup> Bepridil was placed in the pocket using the alignment to 1LXF for system 4B. We generated the starting structures for all the systems based on NMR structure of N-domain of TnC and the X-ray structure of cardiac troponin.

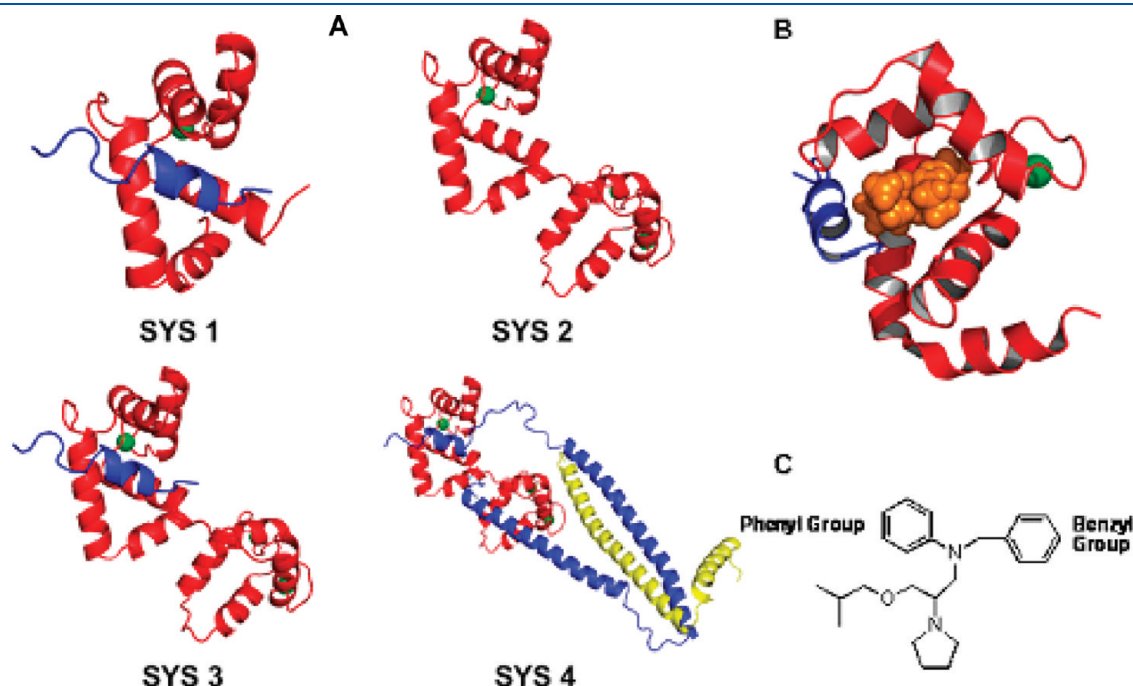


**Figure 2.** (A) Components of cardiac troponin used for four systems. TnC is in red, TnI is in blue, and TnT is in yellow, and calcium ions are green spheres. SYS 1: TnC<sub>1–89</sub>, TnI<sub>147–163</sub>. SYS 2: TnC<sub>1–161</sub>. SYS 3: TnC<sub>1–161</sub>, TnI<sub>147–163</sub>. SYS 4: TnC<sub>1–161</sub>, TnI<sub>31–163</sub>, TnT<sub>183–288</sub>. (B) The NMR structure of the complex composed of the N-domain of TnC<sub>1–89</sub> in red, the switch segment of TnI<sub>147–163</sub> in blue, and bepridil in orange. (PDB ID: 1LXF). (C) The structure of bepridil.

Table 1. Molecular Dynamics Simulation Summary

system	components	ligand	simulation time (ns)
1A	TnC(1–89), TnI(147–163)	none	12.0
1B	TnC(1–89), TnI(147–163)	bepridil	12.0
2A	TnC(1–161)	none	12.0
2B	TnC(1–161)	bepridil	12.0
3A	TnC(1–161), TnI(147–163)	none	11.9
3B	TnC(1–161), TnI(147–163)	bepridil	9.6
4A	TnC(1–161), TnI(31–163), TnT(183–288)	none	12.0
4B	TnC(1–161), TnI(31–163), TnT(183–288)	bepridil	12.0

In addition, the alignment of 1LXF (the NMR structure of N-domain of TnC with bepridil bound) and the N-domain of TnC in 1J1D (the X-ray structure of cardiac troponin) indicated that bepridil binding causes minor conformational changes; the root-mean-square coordinate deviation (rmsd) of the alignment is about 2.5 Å. This indicated that the alignments we used to generate the starting structures in this work are reasonable.

All the four systems were neutralized and explicitly solvated using TIP3P waters in a rectangular box with a minimum distance of 14 Å from the protein to the wall of the box. The MD simulation for SYS 4A was carried out previously to investigate the difference from skeletal troponin.<sup>15</sup> In this work, we analyzed the simulation on cardiac troponin without bepridil again to study the impact of bepridil binding.

**Simulation Details.** Computations including the minimization and MD simulations for the systems were performed on a 128-processor Altix 4700 at East Carolina University. Calculations were carried out using AMBER's all-atom force field as implemented in AMBER 9 software.<sup>16</sup> The SANDER module of AMBER program was used for the computation. Simulations were carried out under periodic boundary conditions with a cutoff of 10 Å to truncate the VDW interactions. The particle-mesh Ewald method<sup>17–20</sup> was used to treat the long-range electrostatic contribution to the force field. The SHAKE algorithm<sup>21</sup> was applied to constrain the hydrogen atoms and allow the usage of longer step size of 1.5 fs.

All the systems were energy minimized before each simulation. A restrained minimization was first performed on the solvent while keeping the protein fixed; then the entire system was minimized. The minimized systems were warmed for 20 ps to a final temperature of 300 K. Then constant pressure dynamics (NPT) was performed on the system for about 300 ps at 1 atm until the density of the systems was stabilized. Finally, constant volume dynamics (NVT) was performed on each of the systems. The starting and final coordinates of each system are available upon request.

The empirical binding affinities of bepridil within the hydrophobic pocket of TnC and calcium in the binding loop of TnC were analyzed by the molecular mechanics-Poisson–Boltzmann surface area (MMPBSA) method<sup>22–24</sup> integrated in AMBER 9.<sup>16</sup> In the MMPBSA analyses, the entropic term was not calculated, since the ligand bindings only cause major conformational changes at the common part of all the systems, namely the N-domain of TnC<sub>1–89</sub>. The entropic term among the four systems should be similar.

**Proteins.** Myosin<sup>25</sup> and actin<sup>26</sup> were isolated from rabbit back muscle. Bovine cardiac troponin<sup>27</sup> and tropomyosin<sup>28</sup> were prepared from left ventricles. Human cardiac troponin was expressed in *E. coli*.<sup>26</sup> Human cardiac TnT2 subcloned into

psBETA vector was expressed in freshly transformed BL21-(DE3)pLysS cells (Carlsbad, CA) and purified as previously described.<sup>29</sup> Human cardiac TnI and TnC were subcloned into pET3d vector (gift from K. Jaquet) and were coexpressed in freshly transformed BL21(DE3)pLysS cells and selected with ampicillin and chloramphenicol. Bacteria were harvested and resuspended in 6 M Urea, 1 mM EDTA, 20 mM Tris-HCl pH 8.0, 5% sucrose, 0.2 mg/mL lysozyme, and protease inhibitor cocktail (Mannheim, Germany) and allowed to incubate overnight at 4 °C after an initial 15 min at room temperature. The suspension was sonicated and the supernatant was loaded on a SP Sepharose High Performance 16/10 column in 6 M urea, 1 mM EDTA, and 20 mM Tris-HCl pH 8.0. Proteins were eluted with a 0–0.5 M NaCl gradient. Nonbound fractions were used for the preparation of TnC. Fractions containing TnI were then passed over a 20 mL DEAE Sephacel column before going over a SP Sepharose High Resolution column for final purification. Crude TnC from the SP column was loaded on a DEAE Sephacel column and eluted with a 0–0.5 M NaCl gradient. For final purification, TnC fractions were loaded on a phenyl Sepharose column in 1 M NaCl, 20 mM Tris-HCl pH 8.0, 0.5 mM CaCl<sub>2</sub>, and 1 mM dithiothreitol and then eluted by replacing the CaCl<sub>2</sub> in the buffer with 1 mM EDTA.

Human cardiac troponin was reconstituted following the previously described protocol<sup>30</sup> with some modifications. TnT2, TnI, and TnC were mixed at a 1:1:1.2 molar ratio and a Protein Pak DEAE 15HR column was used for final purification with start buffer of 0.1 M NaCl, 20 mM Tris-HCl pH 8.0, and 5 mM MgCl<sub>2</sub>. Troponin was eluted with a 0.1–1.0 M NaCl gradient in the same buffer.

**Assays.** ATPase activities were measured by the release of <sup>32</sup>Pi from γ-<sup>32</sup>P labeled ATP (GE Healthcare, Boston, MA) using four time points to establish each initial rate.<sup>31</sup>

The rate of calcium detachment was measured by changes in Quin 2 (Invitrogen, Carlsbad, CA) fluorescence using a DX17. MV/2 sequential mixing stopped flow spectrofluorometer (Applied Photophysics, Leatherhead, UK). The excitation wavelength was 330 nm, and the emission was collected through a Schott 370 nm high-pass filter (transmission midpoint of 400 nm). The temperature was maintained at 4 or 20 °C with a circulating water bath. The basic reaction buffer (100 mM KCl, 20 mM MOPS, pH 7.0, 1 mM dithiothreitol) was passed through a Chelex-100 column (Bio-Rad, Hercules, CA) to lower the free calcium concentration. TnC, the TnC–TnI complex, or whole troponin was in the basic reaction buffer containing 30 μM CaCl<sub>2</sub>. Those protein mixtures were rapidly mixed with equal volumes of the basic buffer containing 60 or 120 μM Quin 2. The increase in fluorescence was generally fit with a biexponential function to obtain apparent rate constants. Control experiments



done in the absence of troponin showed that binding of Quin 2 to the free probe was too fast to measure under these conditions. Furthermore, there was no significant photobleaching of the Quin 2 over 0.5 s. The same concentration of bepridil (Sigma, St. Louis, MO) was present in both syringes to avoid changes resulting from bepridil detachment from troponin. Bepridil was dissolved in 100% ethanol to give a 25 mM stock and then diluted to 5 mM in water prior to adding to the reactions. The concentration of bepridil was determined spectrophotometrically at 296 nm with an extinction coefficient of  $3544 \text{ cm}^{-1} \text{ M}^{-1}$ .<sup>32</sup> The concentration of ethanol was held constant at 0.95% in all assays as this concentration of ethanol, by itself, was found to depress the rate of calcium release by 23%. It was equally important to keep the ethanol concentration constant in ATPase assays.

### III. COMPUTATIONAL RESULTS

Table 1 shows the NVT simulations performed on the four different systems. All simulations were carried out for at least 10 ns to ensure equilibrium. The stability of each simulation was determined by the stability of root-mean-square coordinate deviation of main-chain atoms and the maintenance of a constant average temperature. The B-factor of each residue in each system with and without bepridil was calculated using “atomicfluct” of “ptraj” in the Amber program based on the equilibrated simulations. Prior to the B-factor calculation using “atomicfluct”, the calculation with “rms” of ptraj was performed to remove the rot and tran motions from each step. The B-factors of the backbone atoms of SYS 4A and SYS 4B are shown in Figure 3. The calculated B-factors of SYS 4 were generally consistent with the X-ray B-factors, except for the N-terminus helix (H1, TnT<sub>200–222</sub>) of the incomplete TnT and the N domain of cTnC (TnC<sub>1–89</sub>). The calculated high B-factor of the incomplete TnT helix is due to the fact that during simulation the incomplete TnT helix of cTn is very flexible and gradually loses its secondary structure. The calculated high B-factor of the N-domain of cTnC may be due to the fact that this domain is connected with the C-domain of TnC in cTn by a loop linker and is flexible during simulation. The overall consistency of the calculated B-factor and the X-ray B-factor indicated that the molecular dynamics simulations we performed were appropriate. Based on the simulation trajectory data, the effect of bepridil binding was predicted.

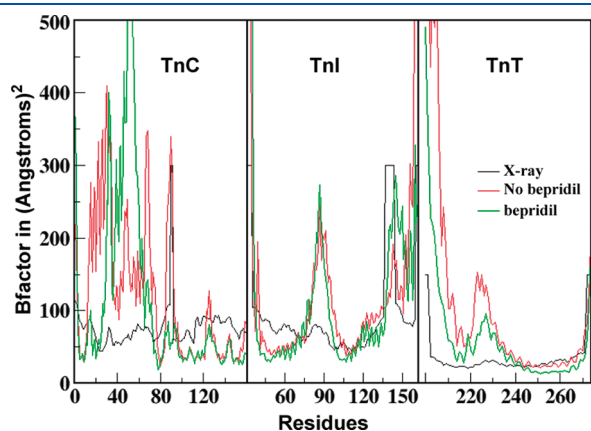


**Figure 3.** Calculated B-factor of SYS 4 with (green) and without bepridil<sup>15</sup> (red), and the X-ray B-factors<sup>13</sup> (black).

**Bepridil Binding.** Early experimental studies have found a 10-fold decrease in bepridil binding constant in going from isolated cTnC to the cTnC·TnI complex. The dissociation constant increased from a  $K_D$  of 10 to  $140 \mu\text{M}$ , respectively.<sup>10,33</sup> Moreover, a structural study of bepridil binding to isolated cTnC found 3 bepridil molecules bound to both the N and C domain pockets of TnC<sup>9</sup> while only a single bepridil was bound to the TnC–TnI complex.<sup>12</sup>

Based on the simulation trajectory data generated for each of the four systems, bepridil binding affinities were estimated using the MMPBSA approach assuming one bepridil was bound per TnC in all cases. The results, shown in Table 2, do not reflect the experimentally observed weakening of bepridil binding in the presence of TnI. The apparent binding affinities for systems 1, 3, and 4 are quite similar. In the case of isolated TnC in system 2, the affinity of the specific binding to the hydrophobic pocket is actually predicted to be weaker than in the more complex systems. Although the large complex, SYS 4, does not have the complete TnI subunit, it does include the switch segment of TnI which binds to hydrophobic pocket. Since bepridil binds to the N-domain of TnC, the direct effects of TnI binding to bepridil can be observed with a structure of a system with the switch segment of TnI. Our differences from the experimental values may result from effects resulting from the other two bepridil molecules bound to isolated TnC that were not present in our simulations.

The bepridil binding energy change between SYS 1 and SYS 3 is within the error range. Thus, the C-domain of TnC may not have a direct effect on N-domain binding of bepridil. By comparing the bepridil binding energies between SYS 3 and SYS 4, it also appears that TnT and TnI long helices present in the structure do not play a role in the binding of bepridil. Hence, the major changes in binding energies of the different systems occur with the presence of the TnI switch segment (TnI<sub>147–163</sub>). SYS 2 and 3 only differ structurally with the presence of the switch segment of TnI but binding energy changes with a larger nonbonded contribution from van der Waals forces.

**Calcium Binding.** Calcium binding to troponin triggers muscle contraction. Calcium-binding affinities were estimated using the MMPBSA approach for the different systems as shown in Table 3. The low-affinity site (site II) has been reported to bind calcium on the order of  $10^6 \text{ M}^{-1}$  in isolated TnC and shown to increase by an order of magnitude once in the troponin complex.<sup>34</sup> Our results in Table 3 also show an increase in binding affinity when comparing the site II binding energies of the isolated TnC (SYS 2A,  $-67.69 \text{ kcal/mol}$ ) and the complex (SYS 4A,  $-115.76 \text{ kcal/mol}$ ).

Bepridil has been reported to enhance calcium binding. Bepridil was shown to delay the rate of calcium release from the low-affinity calcium-specific site in the N-domain of TnC in

**Table 2.** Predicted Bepridil-Binding Affinities (kcal/mol) by MMPBSA

complex	$E_{\text{ele}}$		$E_{\text{VDW}}$		$E_{\text{sol}}$		$\Delta G$	
	mean	STD	mean	STD	mean	STD	mean	STD
SYS 1B	−4.00	1.46	−40.77	3.19	12.50	2.44	−32.27	3.45
SYS 2B	−1.82	1.78	−36.54	3.23	9.52	2.97	−28.85	3.64
SYS 3B	−2.88	1.57	−46.14	2.98	14.23	2.92	−34.79	3.73
SYS 4B	−0.27	1.80	−49.43	3.69	13.82	3.53	−35.88	3.56

**Table 3.** Estimated Calcium-Binding Affinities (kcal/mol) by MMPBSA

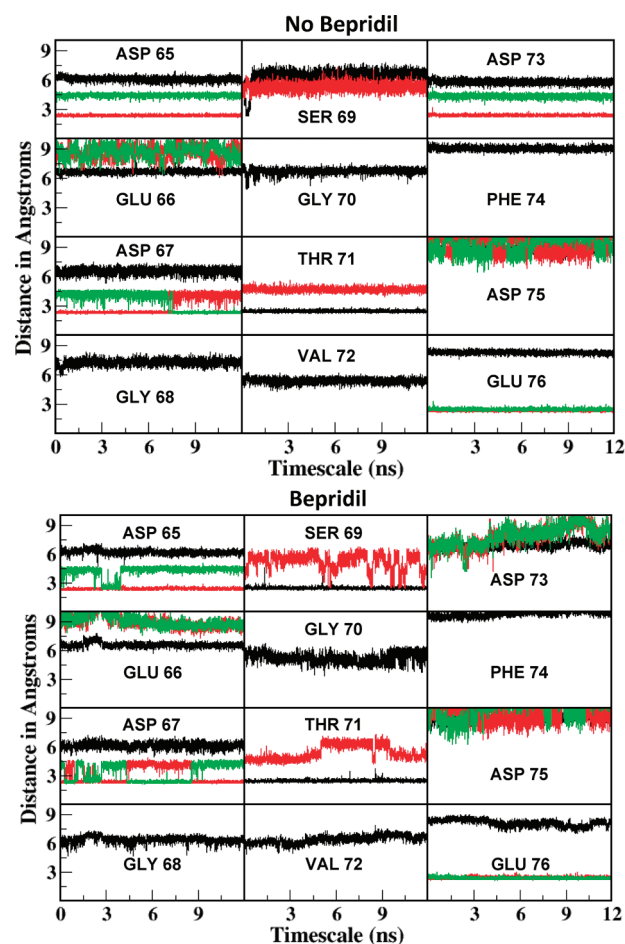
complex	ligand	site II	
		mean	STD
SYS 1A	none	−113.2	10.83
SYS 1B	bepridil	−118.26	15.61
SYS 2A	none	−67.69	5.83
SYS 2B	bepridil	−108.95	20.13
SYS 3A	none	−133.65	15.49
SYS 3B	bepridil	−125.16	11.18
SYS 4A	none	−115.76	9.43
SYS 4B	bepridil	−108.86	20.96

the isolated system.<sup>11</sup> Simulations of SYS 2 with the isolated TnC showed a similar increase in the calcium sensitivity of N-domain site upon bepridil binding (Table 3). Interestingly, calcium binding energies for the N-domain site in the 3-subunit complex in SYS 4 did not show a significant change with the addition of bepridil in the complex. Although experiments demonstrated increased force and calcium sensitization with bepridil in muscle fibres, the effect of bepridil was lower at higher concentrations of calcium.<sup>10</sup> Since the structure used in SYS 4 is based on the calcium saturated X-ray structure of cardiac troponin, bepridil's calcium sensitizing activity may be lowered as seen in the simulation.

In addition, we noticed a decrease in affinity for the C-domain sites in TnC with the addition of bepridil to the N-domain of SYS 4. This suggested that bepridil may have long-range effects that involve changing interactions in the C-domain of TnC.

Our results can be explained more elaborately by considering the distribution of actin–tropomyosin–troponin among the three possible regulatory states. The degree of activity increases as the fraction of actin–tropomyosin–troponin in the active state increases. Since regulated actin is highly cooperative, troponin should have three structures that correspond to the three states of actin. Changes in ligand binding to TnC (TnI or calcium) will affect the structure of troponin and change the distribution of states. The change in state distributions should be reflected in a change in calcium affinity. However, lack of structural data prevented us from identifying the exact structure of the intermediate or active states of troponin. In SYS 2A (isolated TnC) it is known that in cardiac troponin, the lack of TnI keeps the hydrophobic pocket in the closed conformation.<sup>12</sup> That may indicate that in the absence of TnI a greater fraction of TnC is in the inactive state even at saturating calcium. With bepridil present, the calcium affinities of N- and C-domains increase, suggesting a shift to the intermediate or active state. That is, because calcium stabilizes the intermediate state, that state must have the highest calcium affinity. Adding TnI to TnC (comparing SYS 2A to 3A or 2A to 4A) increases calcium affinities of both N and C domain. This shows that the troponin complex is shifting to a more intermediate or active state.

We believe that the SYS 4A structure is not that of the fully active state. That is,  $\text{Ca}^{2+}$  alone gives a distribution of states dominated by an intermediate state.<sup>35</sup> Full activation, in solution, requires additional binding of rigor-type myosin.<sup>36,37</sup> With bepridil it may shift to an even lesser active form (intermediate or inactive) that does not change calcium affinities in the

**Figure 4.** Calcium coordination distances between two TnC complex systems of no bepridil (SYS 4A)<sup>15</sup> and bepridil (SYS 4B) at site II. The backbone oxygens are shown in black, whereas the side-chain oxygens are shown in red (OG/OD1/OE1) and green (OD2/OE2).

N-domain but decreases calcium affinities in the C-domain. Bepridil seems to be stabilizing the transition from the inactive to intermediate or active to intermediate state.

The calcium coordination at site II was studied to learn more about how bepridil may affect  $\text{Ca}^{2+}$  affinity. The distances between each oxygen around the binding loop of site II and calcium were analyzed for SYS 4B (Figure 4B) and compared with that of SYS 4A (Figure 4A).<sup>15</sup> Calcium–oxygen distances below 3 Å were considered as coordinating distances. In the system without bepridil (4A) and with bepridil (4B), six oxygens from the protein ligands were coordinated with calcium with additional oxygen from water (not shown but observed from analysis). The main difference in the ligands is that the no-bepridil system (4A) had ASP 73 OD1 oxygen coordinating with calcium, but this coordination was lost in the bepridil system (4B). Similarly, SER 69 coordinated in SYS 4B but was not seen in the coordination sphere of SYS 4A. In other words, with bepridil the calcium loses coordination with ASP 73 oxygen but gains coordination with SER 69. This may be a reason why we do not see a difference in the binding energies calculated from MMPBSA for site II as one ligand is being replaced by another.

**TnC–TnI Interaction.** Calcium binding changes the interactions among the three components of troponin that permit

Table 4. Interaction (kcal/mol) among Three Components of Troponin by MMPBSA in SYS 4

	ligand	$E_{\text{ele}}$		$E_{\text{vdW}}$		$E_{\text{sol}}$		$\Delta G$	
		mean	STD	mean	STD	mean	STD	mean	STD
TnC–TnI	none	−6151.4	181.15	−210.7	10.98	6106.96	166.21	−255.13	20.71
	bepridil	−5730.3	153.77	−179.1	12.02	5690.81	153.29	−218.57	15.18
TnC–TnT	none	−935.82	83.36	−36.41	4.09	947.48	85.6	−24.75	9.09
	bepridil	−1089.8	92.79	−41.34	5.31	1102.27	88.39	−28.89	11.34
TnT–TnI	none	−170.77	67.66	−203.3	7.62	211.07	66.76	−162.99	11.99
	bepridil	−269.79	57.24	−212.4	7.71	317.54	57.6	−164.6	11.06

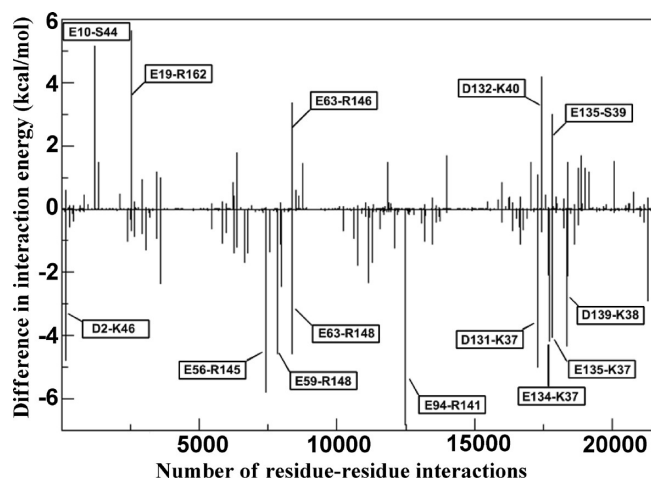


Figure 5. TnC–TnI pairwise residue–residue interaction difference between SYS 4A (no bepridil) and SYS 4B (with bepridil). The prominent differences are labeled with the TnC residue–TnI residue in the box.

muscle contraction to occur. The effect of bepridil on the binding energies among the components was estimated using the MMPBSA approach. Table 4 shows that, with bepridil, the total interaction energy between TnC and TnI decreased by 37 kcal/mol compared to free troponin. Bepridil produced no significant changes in the TnC–TnT or TnT–TnI interactions. In order to classify the residues that were responsible for the change in the TnC–TnI interaction energy, the decomposition energy module using MM-GBSA was used to obtain pairwise residue–residue interaction energies. Having 161 residues in TnC and 133 residues in TnI, we decided to simplify the search and identify the residues by taking an energy difference of each TnC–TnI pair between the no-bepridil (SYS 4A) and bepridil (SYS 4B) form, as shown below:

$$\Delta E = E_{\text{no-bepridil}} - E_{\text{with-bepridil}}$$

$\Delta E$  denotes the TnC–TnI pairwise residue–residue interaction difference,  $E_{\text{no-bepridil}}$  is the TnC–TnI pairwise residue–residue interaction in SYS4A, and  $E_{\text{with-bepridil}}$  is the TnC–TnI pairwise residue–residue interaction in SYS4B. A negative value for  $\Delta E$  indicates that bepridil makes the pairwise interaction less favorable; while a positive value for  $\Delta E$  indicates that bepridil makes the pairwise interaction more favorable. As shown in Figure 5, bepridil increased the number of residue–residue interaction energy differences ( $\Delta E$ ) below 0, demonstrating that bepridil made more residue–residue interactions less favorable. This result was expected as the total interaction between TnC–TnI

subunits was shown to be decreased in the MMPBSA calculation in Table 4.

Figure 5 shows that the destabilized interactions include the N-domain of TnC with the switch segment of TnI and the C-domain of TnC with N-terminal region of TnI. Bepridil weakened the interaction of the N-domain of TnC, including residues E56, E59, and E63, with the N-terminal tail of the switch segment of TnI including residues R145 and R148. Our data are in concord with NMR studies that show a negative cooperativity of binding of bepridil to TnC in the presence of TnI owing to steric and repulsive effects of TnI R148 with the pyrrolidine ring of bepridil.<sup>12</sup> These effects were suggested to cause a reorientation of TnI to fit in the hydrophobic pocket. This reorientation of the TnI switch segment with bepridil may explain the decrease in the interactions with the N-domain of TnC as shown in our simulations.

Bepridil binding to TnC also decreased the interaction energies of residues D131, E134, E135, and D139 of TnC with the residues N-terminal to the H1 helix of TnI (residues K37 and K38). This drop in interaction energies may be a result of bepridil decreasing the  $\text{Ca}^{2+}$  sensitivity of the C-domain sites as seen in our simulation (Table 3). The C-domain calcium sites are also EF-hands that change structurally with the binding of calcium and allow binding of the other segments of troponin including TnI and TnT. With the desensitization of these sites, TnI may be losing some of its interactions with TnC C-domain.

**Correlated Motion.** A cross-correlation analysis<sup>38,39</sup> was applied to investigate the effect of bepridil on the correlated motions within troponin. Strong positive correlations have correlation coefficients or values close to 1 and strong negative correlations have coefficients close to −1. The correlated motions of the large complex (SYS 4B) with bepridil were analyzed and compared with that of SYS 4A<sup>15</sup> without bepridil to explore any differences with the addition of bepridil and are shown in Figure 6. While the correlation patterns are similar for both cases, the pattern with bepridil is more fragmented. That is, the areas of correlation do not appear to run in long contiguous stretches as well when bepridil is present.

In the wild-type system (without bepridil, SYS 4A), the loop residues in the N-domain of calcium-binding site I and site II are highly positively correlated as indicated by the bright yellow spot inside the white square designated as I,II in the left of the Figure 6. This correlation is maintained even though site I is dysfunctional in cardiac troponin. These sites are also correlated in skeletal troponin where both sites are functional and cooperative.<sup>40,41</sup> A similar positive correlation is seen in the C-domain calcium ions and loop residues of site III and site IV as indicated in Figure 6 as III, IV. However, there appears to be minimal correlation between the N-domain sites and C-domain



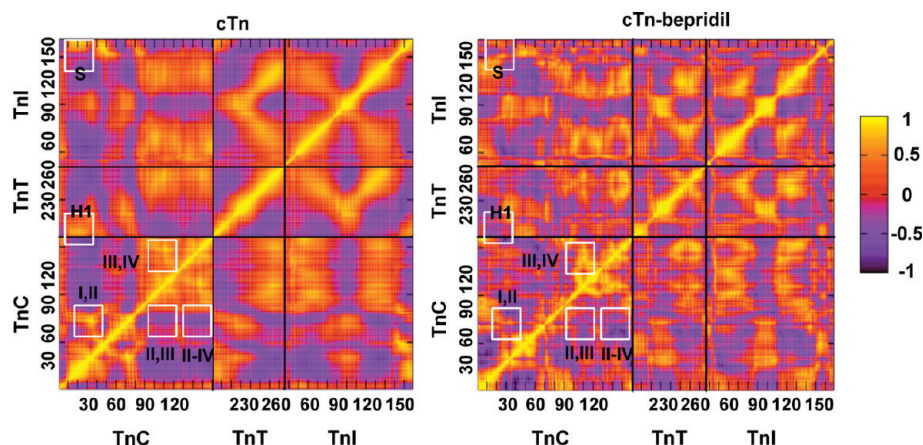


**Figure 6.** Cross-correlation map of cardiac troponin without bepridil (SYS 4A,<sup>15</sup> left) and with bepridil (SYS 4B, right). A strong positive correlation is denoted by 1 and a strong negative correlation is denoted by  $-1$ .

sites. The cross-correlation coefficient values are as follows: sites III and IV with 0.735 showing strong positive correlation, sites II and III with  $-0.320$  showing minimal negative correlation, and sites II and IV with  $-0.496$  showing minimal negative correlation.

With the addition of bepridil in the N-domain of TnC in SYS 4B, the calcium correlation tended to change. The C-domain sites maintained high positive correlations with a correlation coefficient of 0.699; however, site II of the N-domain and site IV of C-domain showed a stronger negative correlation than in the no-bepridil system. The calcium correlation for sites II and IV increased from  $-0.496$  to  $-0.774$  with bepridil while sites II and III correlation remained minimal with a value of  $-0.420$ . Moreover, the loop residues of sites I and II showed lower correlation in the bepridil form than in the no-bepridil form as shown in Figure 6.

In SYS 4A, the N-domain of TnC (cNTnC<sub>1–89</sub>) showed a strong positive correlation with both the N-terminus helix of TnT (H1, TnT<sub>200–222</sub>) and the switch segment of TnI (S, TnI<sub>151–159</sub>). At the same time, the N-domain of TnC showed a negative correlation with the C-domain of TnC, the C-terminus helix of TnT (H2, TnT<sub>226–270</sub>), and particularly with TnI except for the switch segment. The close association of C-domain of TnC (cCTnC<sub>94–161</sub>) with the other domains of troponin can be seen by its strong positive correlations with the large helix of TnT (H2, TnT<sub>226–270</sub>) and the two major helices of TnI (H1, TnI<sub>43–79</sub>, and H2, TnI<sub>91–135</sub>). Bepridil caused two main changes in SYS 4. The N-domain of TnC lost its correlations with the switch segment of TnI (S in Figure 6) and H1 of TnT as shown in Figure 6. Previous experiments on structures including the cNTnC and TnI switch segment suggested a negative cooperativity in the tertiary form (cNTnC·TnI·bepridil) compared to the binary form (cNTnC·TnI) which results in the reorientation of the TnI switch segment that allows the bepridil to bind in the hydrophobic pocket of TnC.<sup>12</sup> The TnI switch segment may lose correlation with the N-domain as it is less associated with TnC in the presence of bepridil.

#### IV. EXPERIMENTAL VERIFICATION

Several experiments were performed to test the computational predictions of bepridil's effects on troponin. We first observed that bepridil had effects on the ATPase activity of myosin S1 even in the absence of troponin. Bepridil reduced the ATPase activity

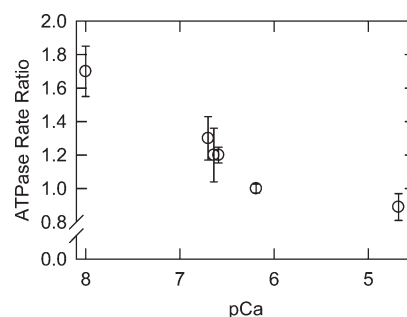


**Figure 7.** Bepridil enhances ATPase activity at low free calcium concentrations. The ratio of rate of ATP hydrolysis (with bepridil/without bepridil) is shown with standard deviations as a function of the pCa. The bepridil concentration is 125  $\mu\text{M}$  with 1% ethanol as a carrier. Conditions: 25  $^{\circ}\text{C}$  with 0.1  $\mu\text{M}$  S1, 20  $\mu\text{M}$  actin, 5.7  $\mu\text{M}$  tropomyosin, and 5.7  $\mu\text{M}$  troponin. The reaction buffer contained 1 mM ATP, 3 mM  $\text{MgCl}_2$ , 20 mM MOPS pH 7, 1 mM dithiothreitol, and sufficient  $\text{CaCl}_2$  and EGTA to reach the target pCa. The ionic strength was adjusted to 62 mM by the addition of KCl. Values in the presence of bepridil were multiplied by 1.23 to correct for inhibition of actin–tropomyosin-stimulated ATPase activity by bepridil.

of S1 alone (0.072/s to 0.059/s), of actin and S1 (1.9/s to 1.6/s), and of tropomyosin–actin and S1 (0.64 to 0.52/s). To correct for these effects when studying the complete system (troponin–tropomyosin–actin and S1), we increased all rates in the presence of bepridil by a factor of 1.23. Figure 7 shows the effect of bepridil on troponin–tropomyosin–actin-activated ATPase activity of myosin S1 in solution. Bepridil had a stimulatory effect at low free-calcium concentrations, but as the calcium concentration was increased this became a mild inhibitory effect. The lack of a stimulatory effect at high calcium saturation has been observed in muscle fibers.<sup>10</sup> Our observation that bepridil affects the troponin complex in the absence of calcium is in contrast to the general view that calcium is required for bepridil binding to TnC.<sup>3</sup> For example, bepridil did not alter isolated TnC–felodipine fluorescence except in the presence of calcium.<sup>10</sup> Furthermore, bepridil produced only small effects on the NMR spectrum of isolated TnC in the absence of calcium.<sup>11</sup> The authors of that study concluded that bepridil binding to isolated TnC is weaker in the absence of calcium. Our experimental system differs from those earlier studies in that we used the

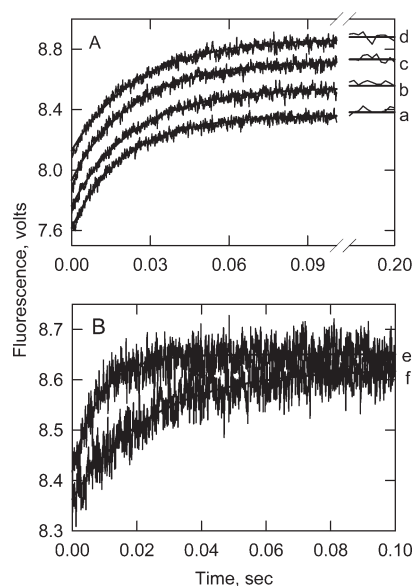


**Figure 8.** Time courses of calcium release from intact cardiac troponin (A) and from the TnI–TnC complex (B).  $\text{Ca}^{2+}$  dissociation was followed by the increase in Quin 2 fluorescence. (A) Calcium release from whole troponin was measured in the absence of bepridil (a) or in the presence of 62.5 (b), 125 (c), and 250 (d)  $\mu\text{M}$  bepridil. (B) Calcium release from the TnI–TnC complex was measured in the absence (e) or presence of 250  $\mu\text{M}$  bepridil (f). Conditions: 3.5  $\mu\text{M}$  troponin or 2.5  $\mu\text{M}$  TnI–TnC, 15  $\mu\text{M}$   $\text{CaCl}_2$ , 100 mM KCl, 20 mM MOPS pH 7, 1 mM dithiothreitol, 60  $\mu\text{M}$  Quin 2, 20  $^\circ\text{C}$ . The time scale for data collection was chosen to observe  $\text{Ca}^{2+}$  release from the low affinity regulatory site.

complete S1–actin–tropomyosin–troponin complex. Furthermore, we used high concentrations of bepridil that would permit low affinity interactions. The ability of bepridil to stimulate activity at low calcium concentrations and to inhibit activity at high calcium concentrations is reminiscent of the effects of some mutations of troponin I that activate the intermediate state of the regulatory complex.<sup>6</sup> It is possible that bepridil stabilizes the intermediate state more than the active state of regulated actin. Any drug designed for treating disorders of the troponin complex should be screened for effects at both high and low free concentrations as changes in the distribution of regulated states can be deleterious to cardiac function.

We tested the prediction that bepridil has little effect on calcium binding to the intact troponin (SYS 4) by measuring the rate of calcium detachment at different bepridil concentrations. Detachment rates should decrease with increasing bepridil concentrations if bepridil strengthens calcium binding. That is, the calcium release rate is inversely related to the calcium affinity in TnC.<sup>11</sup> Figure 8 shows time courses of calcium detachment from the calcium-specific sites of human cardiac troponin. The transients for intact troponin were not affected to a great extent by bepridil while a large difference was seen in the case of the TnI–TnC complex (Figure 8B).

The bepridil concentration dependencies of the calcium dissociation rates for different troponin complexes are shown in Figure 9. The largest effect of bepridil was seen on the human cardiac TnI–TnC complex at 20  $^\circ\text{C}$  (open squares). Bepridil had a 2-fold effect on the TnC complex alone (bovine shown here) in agreement with published reports.<sup>9,42</sup> The human troponin complex was only slightly affected by bepridil at 20  $^\circ\text{C}$  while no effect was seen with bovine cardiac troponin at

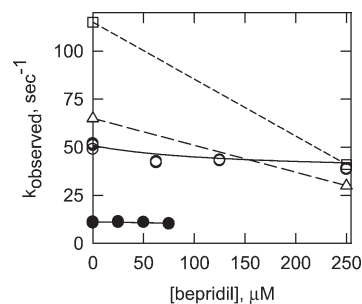


**Figure 9.** Bepridil has little effect on the rate of  $\text{Ca}^{2+}$  dissociation from whole troponin. Calcium dissociation was measured by the increase in Quin 2 fluorescence as shown in Figure 8. Dissociation was measured from the TnI–TnC complex at 20  $^\circ\text{C}$  (squares), TnC alone at 20  $^\circ\text{C}$  (triangles), whole troponin at 20  $^\circ\text{C}$  (open circles), and whole troponin at 4  $^\circ\text{C}$  (solid circles).

4  $^\circ\text{C}$ . These experimental results are consistent with the predictions of the MD simulations of Table 3.

## V. CONCLUSIONS

The computational and experimental approaches in this work suggest that bepridil is not a simple calcium sensitizer. Bepridil enhances the calcium-binding affinity for the isolated TnC but not for the intact troponin complex. Bepridil increases the calcium sensitivity in the isolated TnC by changing the calcium coordination; but in the whole troponin complex, bepridil changes the correlation of the calcium-binding sites by weakening the positive correlation of the calcium-binding sites in the same domain and enhancing the negative correlation of calcium-binding sites at different domains. Bepridil binding decreases the TnC–TnI interaction at both N- and C-domains of TnC. Predicted calcium-binding affinities were verified by the measured  $\text{Ca}^{2+}$ -detachment constants. The  $\text{Ca}^{2+}$ -detachment constants decrease with the increasing of bepridil concentration in the isolated TnC, but was little affected in the whole complex at various bepridil concentrations. Bepridil has a mild inhibitory effect on ATPase activity at high calcium concentration. The results show that molecular dynamics simulations are useful for examining bepridil-induced changes in troponin. As changes in the structure of troponin in different states of activity become defined, the utility of molecular dynamics simulations for predicting drug efficacy will increase.

## AUTHOR INFORMATION

### Corresponding Author

\*E-mail: chalovichj@ecu.edu (J.M.C.); liyu@ecu.edu (Y.L.).  
Phone: (252)744-2973 (J.M.C.); (252)328-9763 (Y.L.).

## ACKNOWLEDGMENT

This work is supported by grants from the National Institutes of Health R01AR044504 to J.M.C. and a Shared Resources Grant from the Brody School of Medicine to J.M.C. and Y.L.

## ABBREVIATIONS:

MOPS, 3-(*N*-morpholino)propanesulfonic acid; S1, myosin subfragment 1; EGTA, ethylene glycol-bis(2-aminoethyl ether)-*N*,*N*,*N*,*N*'-tetraacetic acid; cTn, cardiac troponin; cTnC, cardiac troponin C; TnI, troponin I; TnT, troponin T



## REFERENCES

- (1) Kobayashi, T.; Solaro, R. J. *Annu. Rev. Physiol.* **2005**, *67*, 39–67.
- (2) Haselgro, J. C. *Cold Spring Harbor Symp. Quant. Biol.* **1973**, *37*, 341–352.
- (3) Li, M. X.; Wang, X.; Sykes, B. D. *J. Muscle Res. Cell Motil.* **2004**, *25*, 559–579.
- (4) Chalovich, J. M.; Eisenberg, E. *J. Biol. Chem.* **1982**, *257*, 2432–2437.
- (5) Gomes, A.; Potter, J. *Ann. N.Y. Acad. Sci.* **2004**, *1015*, 214–224.
- (6) Mathur, M. C.; Kobayashi, T.; Chalovich, J. M. *Biophys. J.* **2009**, *96*, 2237–2244.
- (7) Gafurov, B.; Fredricksen, S.; Cai, A.; Brenner, B.; Chase, P. B.; Chalovich, J. M. *Biochemistry* **2004**, *43*, 15276–15285.
- (8) Burhop, J.; Rosol, M.; Craig, R.; Tobacman, L. S.; Lehman, W. J. *Biol. Chem.* **2001**, *276*, 20788–20794.
- (9) Li, Y.; Love, M. L.; Putkey, J. A.; Cohen, C. *Proc. Natl. Acad. Sci. U.S.A.* **2000**, *97*, 5140–5145.
- (10) Solaro, R. J.; Bousquet, P.; Johnson, J. D. *J. Pharmacol. Exp. Ther.* **1986**, *238*, 502–507.
- (11) MacLachlan, L. K.; Reid, D. G.; Mitchell, R. C.; Salter, C. J.; Smith, S. J. *J. Biol. Chem.* **1990**, *265*, 9764–9770.
- (12) Wang, X.; Li, M. X.; Sykes, B. D. *J. Biol. Chem.* **2002**, *277*, 31124–31133.
- (13) Takeda, S.; Yamashita, A.; Maeda, Y. *Nature* **2003**, *424*, 35–41.
- (14) Baker, D.; Sali, A. *Science* **2001**, *294*, 93–96.
- (15) Varughese, J. F.; Chalovich, J. M.; Li, Y. *J. Biomol. Struct. Dyn.* **2010**, *28*, 159–174.
- (16) Case, D. A.; Cheatham, T. E.; Darden, T.; Gohlke, H.; Luo, R.; Merz, K. M.; et al. *J. Comput. Chem.* **2005**, *26*, 1668–1688.
- (17) Kim, K.; Jordan, K. D. *J. Phys. Chem.* **1994**, *98*, 10089–10094.
- (18) Toukmaji, A.; Sagui, C.; Board, J.; Darden, T. *J. Chem. Phys.* **2000**, *113*, 10913–10927.
- (19) Essmann, U.; Perera, L.; Berkowitz, M. L.; Darden, T.; Lee, H.; Pedersen, L. G. *J. Chem. Phys.* **1995**, *103*, 8577–8593.
- (20) Crowley, M. F.; Darden, T. A.; Cheatham, T. E., III; Deerfield, D. W., II. *J. Supercomputing* **1997**, *11*, 255–278.
- (21) Ryckaert, J. P.; Ciccotti, G.; Berendsen, H. J. C. *J. Comput. Phys.* **1977**, *23*, 327–341.
- (22) Wang, J.; Morin, P.; Wang, W.; Kollman, P. A. *J. Am. Chem. Soc.* **2001**, *123*, 5221–5230.
- (23) Wang, W.; Kollman, P. A. *J. Mol. Biol.* **2000**, *303*, 567–582.
- (24) Kollman, P. A.; Massova, I.; Reyes, C.; Kuhn, B.; Huo, S.; Chong, L.; et al. *Acc. Chem. Res.* **2000**, *33*, 889–897.
- (25) Kielley, W. W.; Harrington, W. F. *Biochim. Biophys. Acta* **1960**, *41*, 401–21.
- (26) Eisenberg, E.; Kielley, W. W. *Cold Spring Harbor Symp. Quant. Biol.* **1972**, *37*, 145–52.
- (27) Potter, J. D. *Methods Enzymol.* **1982**, *85*, 241–63.
- (28) Eisenberg, E.; Kielley, W. W. *J. Biol. Chem.* **1974**, *249*, 4742–48.
- (29) Gafurov, B.; Fredricksen, S.; Brenner, B.; Chase, P. B.; Chalovich, J. M. *Biochemistry* **2004**, *43* (48), 15276–85.
- (30) Kobayashi, T.; Solaro, R. J. *J. Biol. Chem.* **2006**, *281* (19), 13471–77.
- (31) Chalovich, J. M.; Eisenberg, E. *J. Biol. Chem.* **1982**, *257*, 2432–37.
- (32) Kleerekoper, Q.; Putkey, J. A. *J. Biol. Chem.* **1999**, *274*, 23932–23939.
- (33) Abusamhadneh, E.; Abott, M. B.; Dvoretzky, A.; Finley, N.; Sasi, S.; Rosevear, P. R. *FEBS Lett.* **2001**, *506*, 51–54.
- (34) Potter, J. D.; Gergely, J. *J. Biol. Chem.* **1975**, *250* (12), 4628–4633.
- (35) Pirani, A.; Xu, C.; Hatch, V.; Craig, R.; Tobacman, L.; Lehman, W. J. *Mol. Biol.* **2005**, *346*, 761–72.
- (36) Eisenberg, E.; Weihing, R. R. *Nature* **1970**, *228* (276), 1092–93.
- (37) Bremel, R. D.; Murray, J. M.; Weber, A. *Cold Spring Harbor Symp. Quant. Biol.* **1972**, *37*, 267–75.
- (38) Ichiye, T.; Karplus, M. *Protein Struct. Funct. Genet.* **1991**, *11*, 205–217.
- (39) Karplus, M.; Ichiye, T. *J. Mol. Biol.* **1996**, *263*, 120–122.
- (40) Teleman, O.; Drakenberg, T.; Forsén, S.; Thulin, E. *J. Biochem.* **1983**, *134*, 453–457.
- (41) Iida, S. *J. Biochem.* **1987**, *103*, 482–486.
- (42) Smith, S. J.; England, P. J. *Br. J. Pharmacol.* **1990**, *100* (4), 779–785.